THEORETICAL STUDIES OF RARE-EARTH NUCLEI LEADING TO $_{50}$Sn-DAUGHTER PRODUCTS AND THE ASSOCIATED SHELL EFFECTS

S. KUMAR

Department of Physics, Chitkara University
(Atal Nagar, Solan-174103, (H.P.) India; e-mail: sushilk17@gmail.com)

UDC 539.1

Cluster decays of rare-earth nuclei are studied with regard for neutron magic shells for $_{50}$Sn nucleus as a daughter product always. The ^{100}Sn and ^{132}Sn radioactivities are studied to find the most probable cluster decays and the possibility, if any, of new neutron shells. For a wide range of parent nuclei considered here (from Ba to Pt), ^{12}C and ^{78}Ni from the ^{112}Ba and ^{210}Pt parents, respectively, are predicted to be the most probable clusters (minimum decay half-life) referring to ^{100}Sn and ^{132}Sn daughters. The ^{22}Mg decay of ^{122}Sm is indicated at the second best possibilty for the ^{100}Sn-daughter decay. In addition to these well-known magic shells ($Z = 50$, $N = 50$ and 82), a new magic shell at $Z = 50$, $N = 66$ (^{116}Sn daughter) is indicated for the ^{64}Ni decay from the ^{180}Pt parent.

1. Introduction

Since the discovery of ^{14}C-decay from ^{223}Ra by Rose and Jones [1] in 1984, many other ^{14}C-decays from other radioactive nuclei (^{221}Fr, ^{221,222,224,226}Ra, ^{223,225}Ac and ^{226}Th) and some 12 to 13 neutron-rich clusters such as ^{20}O, ^{23}F, $^{22,24-26}$Ne, ^{28,30}Mg, and ^{32,34}Si have been observed experimentally for the ground-state decays of translead ^{226}Th to ^{242}Cm parents [2–5], which all decay with the doubly closed shell daughter ^{208}Pb ($Z = 82$, $N = 126$) or its neighboring nuclei. Theoretically, such an exotic natural radioactivity of emitting particles (nuclei) heavier than α-particle was already predicted in 1980 by Săndulescu, Poenaru, and Greiner [6] on the basis of the quantum mechanical fragmentation theory (QMFT) proposed in [7, 8]. To date, ^{34}Si is the heaviest cluster observed with the longest decay half-life ever measured ($\log_{10}T_{1/2}(s) = 29.04$) from ^{238}U parent [9]. Recently, Poenaru *et al.* extended the region of possible emitted clusters $A_c = 14 - 34$ measured in the region of emitters with $Z = 87 - 96$ to superheavy elements up to 124 [10]. In this systematic heavy particle radioactivity, they consider not only the emitted clusters with atomic numbers $2 < Z_c < 29$ but also heavier ones up to $Z_c = Z - 82$, around ^{208}Pb, a doubly magic daughter. For this purpose, they used the Analytical Superasymmetric Fission Model (ASAFM) and estimated the half-life for ^{128}Sn emission from ^{256}Fm (Q-value = 252.129 MeV) and for ^{130}Te emission from ^{262}Rf (Q-value = 274.926 MeV): $\log_{10}T^{\rm Fm}(s) = 4.88$ and $\log_{10}T^{\rm Rf}(s) =$ 0.53, respectively. They are in agreement with experimental values for spontaneous fission [11]: 4.02 and 0.32, respectively.

Keeping in mind the doubly magic nature of the ^{208}Pb daughter, a second island of heavy-cluster radioactivity was predicted on the basis of the ASAFM [12] and the Preformed Cluster Model (PCM) [13] in the decays of some neutron-deficient rare-earth nuclei into ^{100}Sn ($Z = N = 50$) daughter or a neighboring nucleus. Furthermore, Kumar *et al.* [13] predicted another doubly closed ^{132}Sn ($Z = 50$, $N = 82$) daughter radioactivity, for decays of some selective neutron-rich rare-earth nuclei. More recently, an unexpected increase in $E2$ strengths has been reported between the mid-shell isotope ^{116}Sn ($Z = 50$, $N = 66$) and its lighter neighbor, ^{114}Sn [14], and a new shell closure at $N = 90$ is predicted for the ^{140}Sn isotope on the basis of shell model calculations [15]. Experimentally, several unsuccessful attempts [16–19] have been made to measure the ^{100}Sn-daughter radioactivity from the ^{114}Ba parent nucleus produced in the ^{58}Ni+^{58}Ni reaction. Instead, a new phenomenon of intermediate mass fragments (IMFs, with $3 \leq Z \leq 9$), also referred to as "clusters" or "complex fragments" emitted from the excited compound nucleus, was also observed [20]. It is worth mentioning that intermediate mass fragments are mostly found in reactions at intermediate incident energies, where colliding nuclei are broken into many pieces [21].

In this paper, the heavy cluster emissions of rare-earth parents (329 cases) with $_{50}$Sn always as the daughter product are considered. The new experimental mass table [22] and the theoretical masses [23] are used to determine the released energy. Specifically, the emission of various isotopes of C, O, Ne, Mg, Si, S, Ar, Ca, Ti, Cr, Fe, and Ni are considered, respectively, from neutron-deficient to neutron-rich Ba, Ce, Nd, Sm, Gd, Dy, Er, Yb, Hf, W, Os, and Pt parents, with a view to look for ^{100}Sn and ^{132}Sn radioactivities, as well as any other new Sn radioactivity with new shell closures in neutrons. Since the cluster decays are more probable with daughters as magic nuclei, the decay half-lives are expected to drop (be minimum) for the magic daughters. The same idea was utilized earlier for the (spherical) subshell closed $_{40}$Zr daughter [24, 25], including also a brief report of the results on $_{50}$Sn daughter [24]. This calculation is based on PCM [26,27] described briefly in Section 2. The results of our calculations and a summary of our results are presented in Sections 3 and 4.

2. Preformed Cluster Model

The PCM [26] uses the dynamical collective coordinates of mass (and charge) asymmetry, $\eta = (A_1 - A_2)/(A_1 + A_2)$ and $\eta_Z = (Z_1 - Z_2)/(Z_1 + Z_2)$, first introduced in the QMFT [7, 8], which supplement the usual coordinates of relative separation R and deformations β_{2i} $(i = 1, 2)$ of two fragments. Then, in the standard approximation of decoupled R and η motions, in PCM, the decay constant λ or the decay half-life $T_{1/2}$ is defined as

$$\lambda = \frac{\ln 2}{T_{1/2}} = P_0 P \nu_0. \tag{1}$$

Here, P_0 is the cluster (and daughter) preformation probability and P is the barrier penetrability, which refer to the η and R motions, respectively; ν_0 is the barrier assault frequency. The P_0 are the solutions of the stationary Schrödinger equation for η,

$$\left\{-\frac{\hbar^2}{2\sqrt{B_{\eta\eta}}}\frac{\partial}{\partial\eta}\frac{1}{\sqrt{B_{\eta\eta}}}\frac{\partial}{\partial\eta}+V_R(\eta)\right\}\psi^{(\omega)}(\eta) = E^{(\omega)}\psi^{(\omega)}(\eta), \tag{2}$$

which, on proper normalization, gives ω=0,1,2,3.... Equation (2) is solved at a fixed $R = R_a = C_t(= C_1 + C_2)$ (the first turning point of the WKB integral defined below), where C_i are the Süssmann central radii $C_i = R_i - (1/R_i)$ (in fm), with the radii $R_i = 1.28A_i^{1/3} - 0.76 + 0.8A_i^{-1/3}$. Many other formulas for the radius are available (see, e.g., [28]) and widely used in the calculations of barrier heights, which is also a subject of interest for the future study in PCM. We have

$$P_0 = \sqrt{B_{\eta\eta}} \mid \psi^{(0)}(\eta(A_i)) \mid^2 (2/A). \tag{3}$$

The fragmentation potential $V_R(\eta)$ in (2) is calculated simply as the sum of the Coulomb interaction potential, the nuclear proximity potential [29], and the ground state binding energies of two nuclei,

$$V(R_a, \eta) = -\sum_{i=1}^{2} B(A_i, Z_i) + \frac{Z_1 Z_2 e^2}{R_a} + V_P. \tag{4}$$

The proximity potential between two nuclei is defined as

$$V_p = 4\pi\overline{C}\gamma b\Phi(\xi), \tag{5}$$

where γ is the nuclear surface tension coefficient, $\overline{C}$ determines the distance between two points of the surfaces, evaluated at the point of the closest approach, and $\Phi(\xi)$ is the universal function. It depends only on the distance between two nuclei and is given as

$$\Phi(\xi) = -0.5(\xi - 2.54)^2 - 0.0852(\xi - 2.54)^3 \quad \text{for} \quad \xi \le 1.2511,$$

$$= -3.437\exp(-\xi/0.75) \quad \text{for} \quad \xi \ge 1.2511.$$

Here, $\xi = s/b$, i.e., s in units of b, with the separation distance $s = R - C_1 - C_2$; b is the diffuseness of the nuclear surface given by

$$b = \left[\pi/2\sqrt{3}\ln 9\right]_{t_{10-90}}, \tag{6}$$

where t_{10-90} is the thickness of the surface, in which the density profile changes from 90% to 10%. The γ is the specific nuclear surface tension given by

$$\gamma = 0.9517\left[1 - 1.7826\left(\frac{N-Z}{A}\right)^2\right] \text{MeV}\cdot\text{fm}^{-2}. \tag{7}$$

In recent years, many more microscopic potentials became available that takes care various aspects such as the overestimation of a fusion barrier in the original proximity potential and isospin effects. A comparison is also available between all models [30]. As noted above, even modified proximity potentials were also given. We plan to study cluster decays with these new proximity potentials in the near future. Here, Bs are taken from the recent experimental compilation of Audi and Wapstra [22] and, whenever not available in [22], from the calculations of Möller *et al.* [23]. Thus, the full shell effects are contained in our calculations that come from the experimental and/or calculated binding energies. We also note that, for exotic clusters/nuclei with neutron/proton-rich matter, new binding energies are also available [31]. The momentum-dependent potentials and the symmetry energy potential which are found to have a drastic effect at higher densities will not affect decay studies, since these happen at a lower tail of the density [32, 33]. In Eq. (4), the Coulomb and proximity potentials are for spherical nuclei, and charges Z_1 and Z_2 in (4) are fixed by minimizing the potential in the η_Z coordinate. The mass parameters $B_{\eta\eta}(\eta)$, representing the kinetic energy part in Eq. (2), are the classical hydrodynamical masses of Kröger and Scheid [34] used here for simplicity.

The penetrability P is the WKB tunneling integral solved analytically [26] for the second turning point R_b defined by $V(R_b) = Q$-value for the ground-state decay, and the assault frequency ν_0 in (1) is given simply as

$$\nu_0 = (2E_2/\mu)^{1/2}/R_0, \qquad (8)$$

with $E_2 = (A_1/A)Q$, the kinetic energy of the cluster (the lighter fragment), for the Q-value shared between the two products as the inverse of their masses, R_0 is the radius of the parent nucleus, and μ is the reduced mass.

3. Calculations and Results

As already stated in Introduction, the cluster decays of various isotopes of $_{56}$Ba to $_{78}$Pt parents are calculated for the daughter nucleus to be always an isotope of $_{50}$Sn nucleus. For example, for the neutron-deficient $^{110-132}$Ba and neutron-rich $^{144-150}$Ba parents considered here, different isotopes of a carbon cluster would give rise to various isotopes of $_{50}$Sn daughter. This is illustrated in Fig. 1 for the decay half-life $T_{1/2}$ of various C-decays, together with the Q-values, logarithms of the penetrability P and preformation factor P_0, as a function of N_D, the neutron number of $_{50}$Sn daughter. The impinging frequency ν_0 is nearly constant $\sim 10^{21}$ (s^{-1}). All the four quantities Q, P, P_0, and $T_{1/2}$ show the shell effects at magic $N_D = 50$ and 82; the Q, P, and P_0 being large and $T_{1/2}$ small at these numbers. Thus, the most favorable decay is ^{12}C from ^{112}Ba nucleus in the $48 \le N_D \le 70$ region, leaving behind ^{100}Sn as a daughter product, and the ^{14}C cluster from ^{146}Ba in the $72 \le N_D \le 86$ region with ^{132}Sn as a daughter product. This result is same as in [13], where the most probable clusters for ^{100}Sn daughters were obtained as $A_2 = 4n$, $N = Z$, ^{12}C, ^{16}O, ^{20}Ne, ^{24}Mg, and ^{28}Si emitted from the respective Ba to Gd parents, and that these were ^{14}C, ^{20}O, *etc.*, for ^{132}Sn daughter emitted from ^{146}Ba, ^{152}Ce, *etc.*

In the present study, however, the other most probable clusters considered are (isotopes of O, Ne, Mg, Si, S, Ar, Ca, Ti, Cr, Fe, and Ni) from heavier neutron-deficient and neutron-rich rare-earth parents ($^{118-170}$Ce, $^{118-176}$Nd, $^{122-184}$Sm, $^{132-190}$Gd, $^{132-194}$Dy, $^{138-200}$Er, $^{148-200}$Yb, $^{154-208}$Hf, $^{156-208}$W, $^{160-210}$Os, and $^{168-210}$Pt). Interestingly, ^{12}C remains to be the most favorable cluster-decay from ^{112}Ba parent with ^{100}Sn-daughter [13], but, for ^{132}Sn-daughter, the most favorable cluster is now ^{78}Ni from ^{210}Pt, instead of ^{14}C from ^{146}Ba. This is illustrated in Fig. 2,*a* and *c*, respectively, for ^{100}Sn and ^{132}Sn daughters, where the most probable clusters emitted from Ba to Pt parents are plotted. The fact that the most probable cluster ^{78}Ni, arising from Pt parents, occurs at N_D=82 of $_{50}$Sn daughter is illustrated in Fig. 3 for $T_{1/2}$ alone. However, in Fig. 3, in addition to the strong minima at $_{50}$Sn-daughter neutrons N_D=82, a new minimum is also shown to be present at N_D=66 for the $_{50}$Sn daughter, emitting ^{64}Ni cluster from ^{180}Pt parent. This is further illustrated to be true in Fig. 2,*b*. Thus, a new possibility of ^{116}Sn-daughter radioactivity is indicated here. Apparently, other cases of interest in Fig. 2 are the ^{22}Mg decay of ^{122}Sm and ^{50}Ca decay of ^{182}Yb, respectively, with ^{100}Sn and ^{132}Sn as daughters.

Finally, Fig. 4 gives a complete histogram of the decay half-lives $\log_{10}T_{1/2}$(s) as a function of the neutron number N_D of the emitted $_{50}$Sn-daughters with the most probable clusters (minimum $T_{1/2}$ values) from some 329 parents taken from Ba to Pt with mass numbers $A = 110 - 210$. We limited ourselves to $N_D \sim$94, since, for $N_D >$90, the contribution from nuclei heavier than Pt would also become important. Note that, in Fig. 4, the $_{50}$Sn daughter is kept fixed, and all possible clusters are considered from different parents (total 1617 combinations with the $_{50}$Sn daughter and the probable cluster), and then the one with minimum half-life time is plotted. Apparently, the shortest half-life time $\log_{10}T_{1/2}(s) = 2.27$ (with Q-value=22.16 MeV) is obtained for ^{12}C decay of ^{112}Ba. The role of the magic

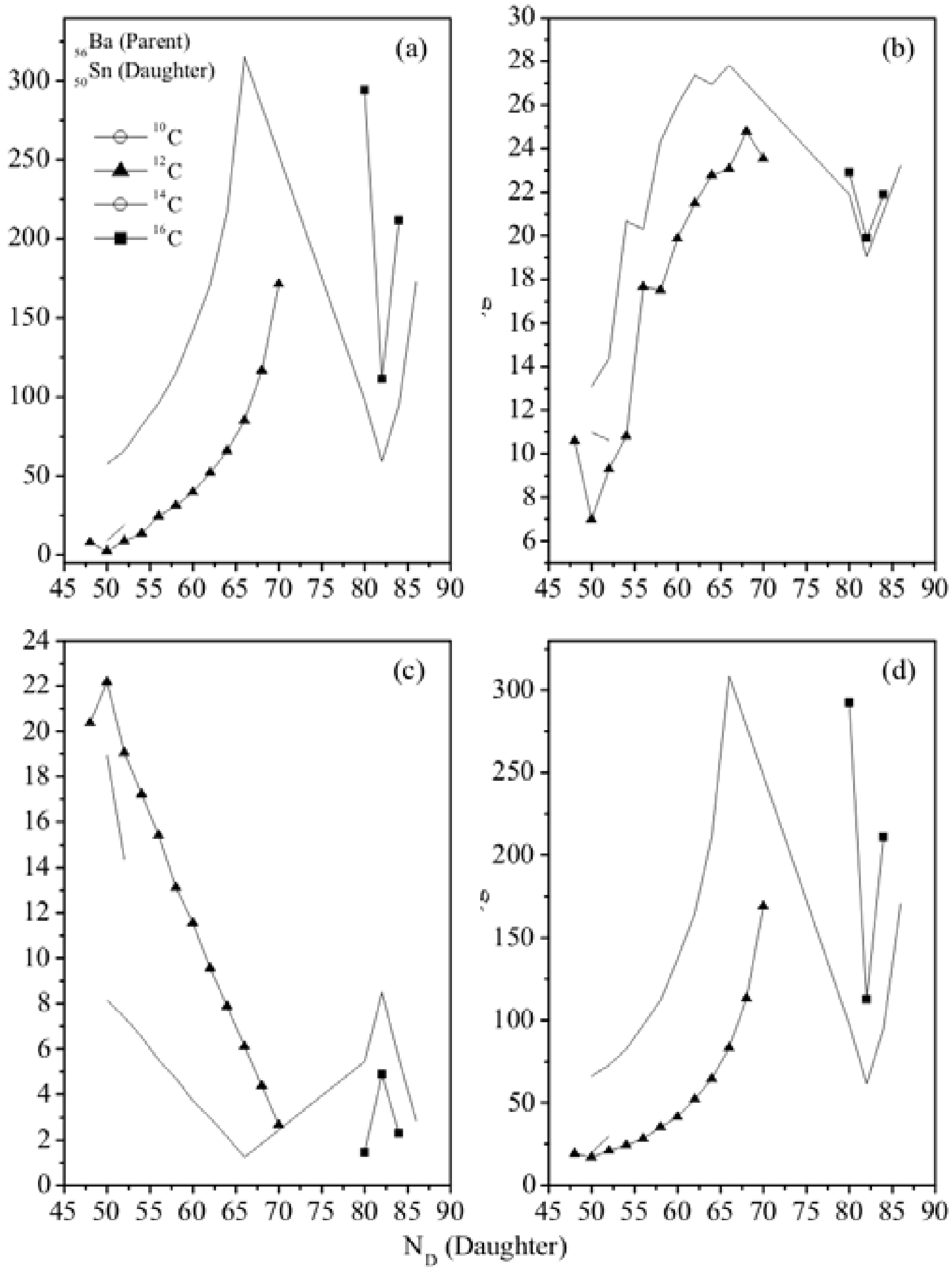

Fig. 1. Decay half-lives $T_{1/2}$ (s) and other characteristic quantities like the preformation factors P_0, Q-values (in MeV), and penetrabilities P of different carbon clusters emitted with $_{50}$Sn daughters from various isotopes of Ba nuclei calculated on the basis of the PCM and plotted as a function of the daughter neutron number N_D

$N_D = 82$ is also evident with a minimum in the histogram at the ^{132}Sn daughter due to the emission of ^{78}Ni cluster from ^{210}Pt parent. The predicted half-life $\log_{10}T_{1/2}(s) = 34.974$ (with a Q-value $= 119.292$ MeV), which is beyond the limit of present-day experiments. Thus, as expected, the strongest shell effects occur at $N_D = 50$ and 82. In addition, another minimum due to ^{64}Ni cluster emitted from ^{180}Pt parents could also be of interest for a closed shell (either spherical and/or deformed) at $N_D = 66$. This minimum is comparable

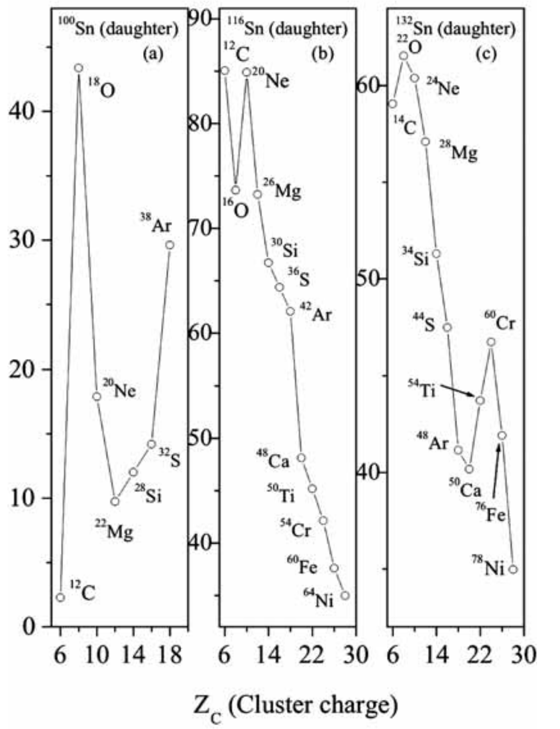

Fig. 2. $log_{10}T_{1/2}(s)$ for the most probable clusters emitted from various Ba to Pt parents with ^{100}Sn (a), ^{116}Sn (b), and ^{132}Sn (c) daughters calculated on the basis of the PCM and plotted as a function of the cluster proton number Z_2. Note the different ordinate-scales are used in these figures

to the $N_D = 82$ case with a predicted decay half-life also of nearly the same value ($\log_{10}T_{1/2}(s) = 34.975$, with a Q-value $= 124.192$ MeV), which is again, by all means, very large for experiments. Note from Fig. 2 that the decay half-life for ^{22}Mg emitted from ^{122}Sm ($log_{10}T_{1/2}(s) = 9.735$) lies in between the values for the ^{12}C decay of ^{112}Ba and ^{78}Ni cluster from ^{210}Pt parent (or ^{64}Ni cluster emitted from ^{180}Pt parent), rather closer to that for the ^{12}C decay of ^{112}Ba.

4. Conclusions

The preformed cluster model is used for the cluster decay calculations with $_{50}$Sn as a daughter nucleus always from various parents of the Ba-to-Pt region. Thus, ^{100}Sn- and ^{132}Sn-daughter radioactivities are look for the most probable clusters (minimum decay half-life time) emitted from the rare-earth parents and the presence of any new neutron magicity. The most probable clusters, respectively, with ^{100}Sn and ^{132}Sn daughters, are predicted to be ^{12}C from ^{112}Ba and ^{78}Ni from ^{210}Pt. The further possibilities with ^{100}Sn and ^{132}Sn daughters are also noticeable in ^{22}Mg and ^{50}Ca clusters emitted from ^{122}Sm and ^{182}Yb parents, respectively, as the second best new cases. In addition, a new shell is indicated at N_D=66 with ^{116}Sn daughter due to ^{64}Ni cluster emitted from ^{180}Pt parent. However, these calculations seem at present to

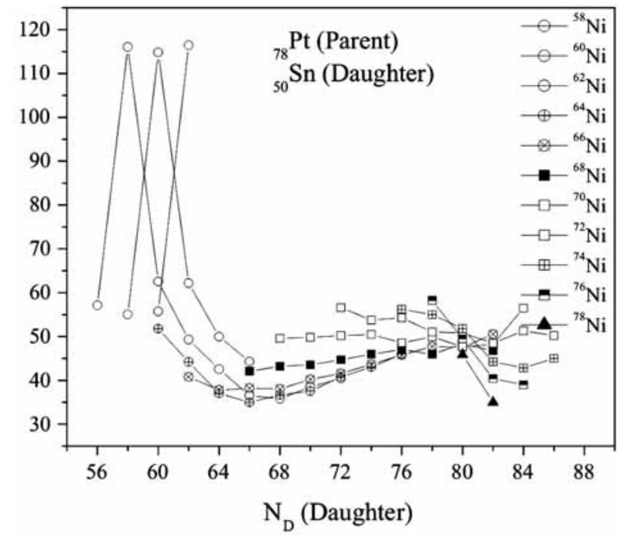

Fig. 3. Same as for Fig. 1, but for $T_{1/2}$ (s) alone, and for different Ni clusters emitted from various Pt parents

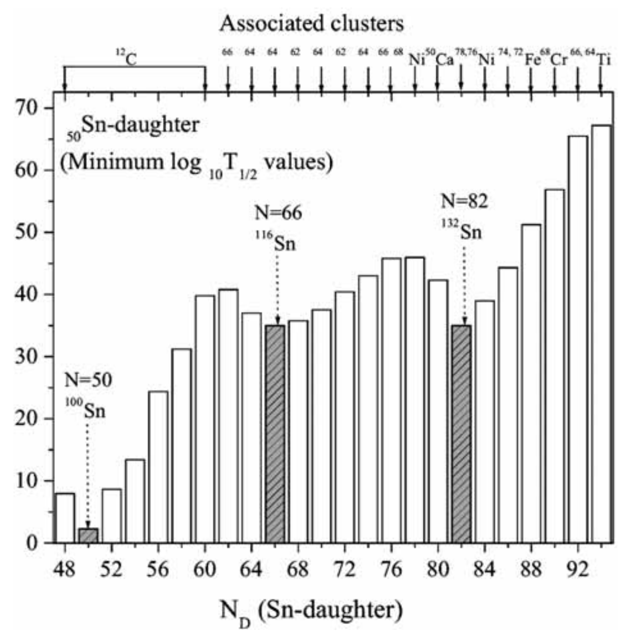

Fig. 4. Histogram of $\log_{10}T_{1/2}$ (s) versus the $_{50}$Sn-daughter neutron number N_D for the most probable clusters emitted from various Ba to Pt parents with $_{50}$Sn as a daughter nucleus always, calculated on the basis of the PCM. The associated clusters are shown on the top panel

be more of an academic interest, since the predicted half-life times, for at least the ^{116}Sn and ^{132}Sn-daughter radioactivities, are too large for experiments.

The author is thankful to Prof. R.K. Gupta for many fruitful discussions.

1. H.J. Rose and G.A. Jones, Nature (London) **307**, 245 (1984).
2. R.K. Gupta and W. Greiner, Int. J. Mod. Phys. E **3**, 335 (1994, Suppl.).
3. R. Bonetti and A. Guglielmetti, in *Heavy Elements and Related New Phenomena*, edited by W. Greiner and R.K. Gupta (World Scientific, Singapore, 1999), Vol. II, p. 643.
4. R. Bonetti and A. Guglielmetti, Roman. Rep. in Phys. **59**, 301 (2007).
5. A. Guglielmetti *et al.*, J. of Phys.: Confer. Series **111**, 012050 (2008).
6. A. Săndulescu, D.N. Poenaru, and W. Greiner, Sov. J. Part. Nucl. **11**, 528 (1980).
7. J. Maruhn and W. Greiner, Phys. Rev. Lett. **32**, 548 (1974).
8. R.K. Gupta, W. Scheid, and W. Greiner, Phys. Rev. Lett. **35**, 353 (1975).
9. R. Bonetti, A. Guglielmetti, V.L. Mikheev, and S.P. Tretyakova, Private communication; and to be published.
10. D.N. Poenaru, R. Gherghescu and W. Greiner, arxiv:1106.3271v1 (2011).
11. D.C. Hoffman, T.M. Hamilton, and M.R. Lane, in *Nuclear Decay Modes* (IOP Publishing, Bristol, 1996), Ch. 10, pp. 393-432.
12. D.N. Poenaru, W. Greiner, and R. Gherghescu, Phys. Rev. C **47**, 2030 (1993); D.N. Poenaru, W. Greiner, and E. Hourani, Phys. Rev. C **51**, 594 (1995).
13. S. Kumar and R.K. Gupta, Phys. Rev. C **49**, 1922 (1994); **51**, 1762 (1995); J. Phys. G: Nucl. Part. Phys. **22**, 215 (1996).
14. J. Walker *et al.*, Phys. Rev. C **84**, 014319 (2011); and references therein.
15. S. Sarkar and M. Saha Sarkar, Phys. Rev. C **81**, 064328 (2010).
16. Yu.Ts. Oganessian, *et al.*, Z. Phys. A **349**, 341 (1994).
17. A. Guglielmetti, *et al.*, Phys. Rev. C **52**, 740 (1995).
18. A. Guglielmetti *et al.*, Phys. Rev. C **56**, R2912 (1997).
19. C. Mazzocchi, *et al.*, Phys. Lett. B **532**, 29 (2002).
20. J. Gomez del Campo *et al.*, Phys. Rev. Lett. **61**, 290 (1988); J. Gomez del Campo *et al.*, Phys. Rev. C **43**, 2689 (1991); **57**, R457 (1998).
21. Y.K. Vermani *et al.*, Nucl. Phys. A **847**, 283 (2011); J. Phys. G: Nucl. Part. Phys. **36**, 105103 (2010); G37 (2010) 015105; Europhys. Lett. **85**, 62001 (2009); R.K. Puri *et al.*, Phys. Rev. C **54**, R28 (1996); J. Comp. Phys. **162**, 245 (2000); Phys. Rev. C **57** (1998)2744; **58**, 320 (1998); J. Singh *et al.*, Phys. Rev. C **62**, 044617 (2000).
22. G. Audi, A.H. Wapstra, and C. Thibault, Nucl. Phys. A **729**, 337 (2003).
23. P. Möller *et al.*, At. Data Nucl. Data Tables **59**, 185 (1995).
24. S. Kumar *et al.*, Symp. on Nucl. Phys., Mumbai (India), Dec. 8-12, Vol. **46B**.
25. S. Kumar *et al.*, J. Phys. G: Nucl. Part. Phys. **36**, 015110 (2009).
26. S.S. Malik and R.K. Gupta, Phys. Rev. C **39**, 1992 (1989).
27. S. Kumar and R.K. Gupta, Phys. Rev. C **55**, 218 (1997).
28. I. Dutt and R.K. Puri, Phys. Rev. C **81**, 064609 (2010); and references therein.
29. J. Blocki, J. Randrup, W.J. Swiatecki, and C.F. Tsang, Ann. Phys. (NY) **105**, 427 (1977).
30. R.K. Puri *et al.*, Phys. Rev. C **45**, 1837 (1992); *ibid* **43**, 315 (1991); *ibid* **47**, 561 (1993); Eur. Phys. J. **23**, 429 (2005); J. Phys. G. **18**, 903 (1992); **18**, 1533 (1992); Eur. Phys. J. A **3**, 277 (1998); **8**, 103 (2000); J. Phys. G. **18**, 1533 (1992); Int. Mod. Phys. E **1**, 269 (1992); Phys. Rev. C **51**, 1568 (1995); J. Phys. G **17**, 1933 (1991); S.S. Malik *et. al.*, Pramana J. **32**, 419 (1989); R.K. Puri, *et al.*, Nucl. Phys. A **575**, 733 (1994); I. Dutt *et. al.*, Phys. Rev. C **81**, 044615 (2010); **81**, 064608 (2010); **81**, 047601 (2010).
31. S. Goyal *et al.*, Phys. Rev. C **83**, 047601 (2011).
32. A.D. Sood *et al.*, Phys. Rev. C **70**, 034611 (2004); *ibid* **79**, 064618 (2009); *ibid* C **73**, 067602 (2006); *ibid* J. Phys. G **37**,) 085102 (2010.
33. Y. Vermani *et al.*, Phys. Rev. C **79**, 064613 (2009); S. Kumar *et al.*, Phys. Rev. C **78**, 064602 (2008); *ibid* **81**, 014601 (2010); *ibid* **81**, 014611 (2010); R. Chugh *et al.*, Phys. Rev. C **82**, 014603 (2010); A.D. Sood *et al.*, Eur. Phys. J. A **30**, 571 (2006).
34. H. Kröger and W. Scheid, J. Phys. G **6**, L85 (1980).

Received 07.07.11

ТЕОРЕТИЧНЕ ДОСЛІДЖЕННЯ РІДКОЗЕМЕЛЬНИХ ЯДЕР З $_{50}$Sn ДОЧІРНІМИ ПРОДУКТАМИ І СУПУТНІ ОБОЛОНКОВІ ЕФЕКТИ

С. Кумар

Р е з ю м е

Досліджено кластерні розпади рідкоземельних ядер з урахуванням нейтронних магічних оболонок з $_{50}$Sn ядром як дочірнім продуктом. Розглянуто радіоактивність ^{100}Sn і ^{132}Sn для визначення найбільш імовірних кластерних розпадів і, якщо це можливо, нових нейтронних оболонок. Для широкого діапазону материнських ядер (від Ba до Pt) передбачається, що ^{12}C і ^{78}Ni з материнських ядер ^{112}Ba і ^{210}Pt, відповідно, є найбільш імовірними кластерами (з мінімальним часом напіврозпаду), які відповідають дочірнім ядрам ^{100}Sn і ^{132}Sn. Розпад ^{122}Sm з продуктом ^{22}Mg відзначений як друга найкраща можливість для розпаду з ^{100}Sn дочірнім ядром. Крім добре відомих магічних оболонок ($Z = 50$, $N = 50$ і $N = 82$), нова магічна оболонка з $Z = 50$, $N = 66$ (дочірнє ядро ^{116}Sn) вказана для розпаду материнського ядра ^{180}Pt по каналу з ^{64}Ni.

ТЕОРЕТИЧЕСКОЕ ИССЛЕДОВАНИЕ РЕДКОЗЕМЕЛЬНЫХ ЯДЕР С $_{50}$Sn ДОЧЕРНИМИ ПРОДУКТАМИ И СОПУТСТВУЮЩИЕ ОБОЛОЧЕЧНЫЕ ЭФФЕКТЫ

С. Кумар

Р е з ю м е

Исследованы кластерные распады редкоземельных ядер с учетом нейтронных магических оболочек с $_{50}$Sn ядром как дочерним продуктом. Рассмотрена радиоактивность ^{100}Sn и ^{132}Sn для определения наиболее вероятных кластерных распадов и, если это возможно, новых нейтронных оболочек. Для широкого диапазона материнских ядер (от Ba до Pt) предсказывается, что ^{12}C и ^{78}Ni из материнских ядер ^{112}Ba и ^{210}Pt, соответственно, являются наиболее вероятными кластерами (с минимальным временем полураспада), которые отвечают дочерним ядрам ^{100}Sn и ^{132}Sn. Распад ^{122}Sm с продуктом ^{22}Mg отмечен как вторая наилучшая возможность для распада с ^{100}Sn дочерним ядром. Кроме хорошо известных магических оболочек ($Z = 50$, $N = 50$ и $N = 82$), новая магическая оболочка с $Z = 50$, $N = 66$ (дочернее ядро ^{116}Sn) указана для распада материнского ядра ^{180}Pt по каналу с ^{64}Ni.